Further Improving Coulombic Efficiency and Discharge Capacity in $LiNiO_2$ Material by Activating Sluggish ~3.5 V Discharge Reaction

Changgeun Bae[1], Nicolas Dupre[2], and Byoungwoo Kang[1]*
1 POSTECH - Pohang University of Science and Technology
2 IMN - Institut des Matériaux Jean Rouxel

ABSTRACT: The electrochemical activity of LiNiO2 at the initial cycle and factors affecting its activity were understood. Even though LiNiO2 can achieve almost theoretical charge capacity, it cannot deliver the theoretical discharge capacity that would result in low 1st Coulombic efficiency (CE). For different upper cut-off voltages at 4.3 and 4.1 V, the 1st CE barely increases. Given that the H2−H3 phase transition occurs at ~4.2 V, the low 1st CE is not caused by this phase transition but is a result of the additional 3.5 V discharge reaction, which is kinetically limited and thereby not activated even at a reasonable current density. We found out that the several phase transitions during charge/discharge in LiNiO2 barely affect the 3.5 V reaction. Under galvanostatic intermittent titration technique (GITT) conditions, LiNiO2 can achieve ~250 mAh/g of discharge capacity and 100% CE even with the 4.3 V cut-off voltage by fully activating the 3.5 V reaction. Using neutron diffraction and 6Li nuclear magnetic resonance (NMR) measurements, the sluggish kinetics of the 3.5 V reaction can be ascribed to difficult insertion of Li at the end of the discharge because this reaction can be accompanied by the rearrangement of cations or local structure change in the structure. To achieve high discharge capacity in LiNiO2 with the 4.3 V cut-off voltage, this 3.5 V sluggish reaction should be improved. The finding and understanding underlying the mechanism of the electrochemical activity will stimulate further research on high-capacity Ni-rich layered materials for high-performance Li-ion batteries.

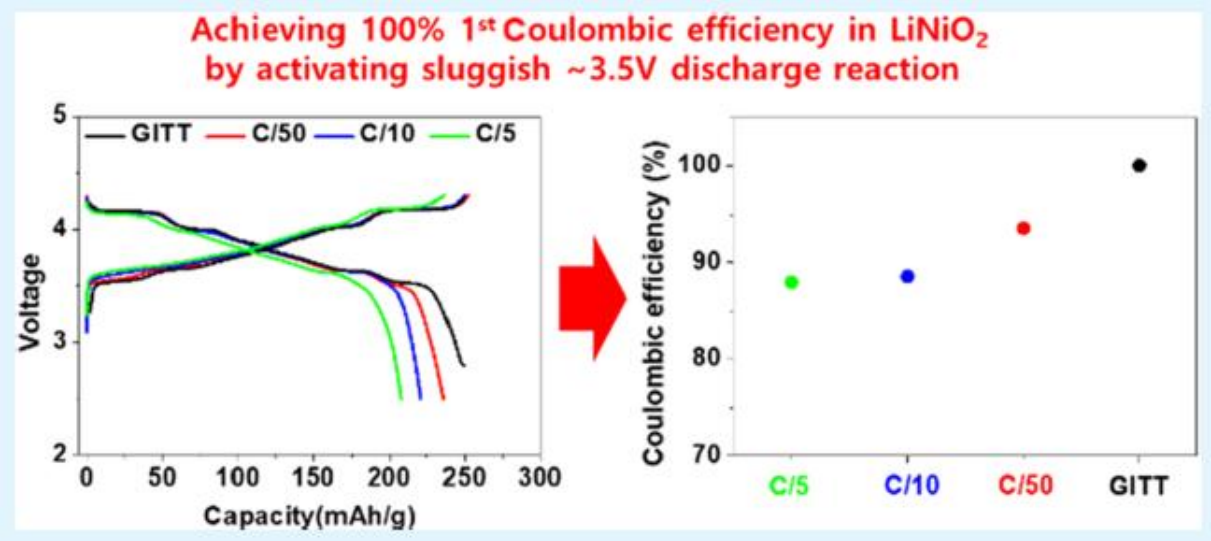

KEYWORDS: high Ni-rich materials, LiNiO2, Coulombic efficiency, discharge reaction at ~3.5 V, cation rearrangement

1. INTRODUCTION

Many attempts to increase the energy density and reduce the production cost of the Li-ion battery (LIB) have been performed in both business and academic fields since LIB is

commercialized. Using LiCoO2 (LCO) as a cathode material and graphite as an anode material, the early LIB has been applied mostly in portable devices. But a strong demand for high energy density in LIB has been increased for deploying extended-range electric vehicles (EVs) as the electric vehicle (EV) market grows. As the demand for high energy density LIB increases, the conventional LCO material, with a lower practical capacity, has been replaced due to its structure instability after >50% delithiation and the substantial increase of the price of Co.1 Li-rich layered oxide and Ni-rich layered oxide were considered as candidates for replacing LCO because of their higher energy density2,3 and already Ni-rich layered oxide is used in the EV system. Ni-based layered materials such as LiNi1 −x−yMnxCoyO2 (NMC) and Li- Ni0.8Co0.15Al0.05O2 (NCA) have been of great interest because they can achieve high reversible capacity by only substituting Co with Ni. To further increase the energy density in Ni-based layered materials, the amount of Ni in the materials gets increased by reducing other transition metals such as Co and Mn because the Ni redox reaction determines the achievable capacity of the electrode materials.4 As the Ni content increases in NMC and NCA materials, their electrochemical properties and structural changes via phase transformation behaviors during charge/discharge are increasingly similar to LiNiO2, an end member of Ni-rich electrode materials.5 For example, as the Ni amount increases, multiple phase transitions, including the H2−H3 phase transition at the end of charge, which can cause severe structural changes, are observed during charge/discharge and the thermal stability of the fully delithiated phase gets worse with the oxygen release.6,7 Also, the Ni-rich layered materials (Ni > 80%) exhibit low Coulombic efficiencies at the 1st cycle that are less than 90%.8−11 This indicates that the discharge capacity does not increase along with the charge capacity even though the Ni content increases. To achieve the increase in the discharge capacity in Ni-rich layered materials, the electrochemical properties of Ni-rich layered materials at the 1st cycle should be understood. Therefore, the understanding of the electrochemical activity of LiNiO2 can greatly help solving these problems of Ni-rich layered materials.

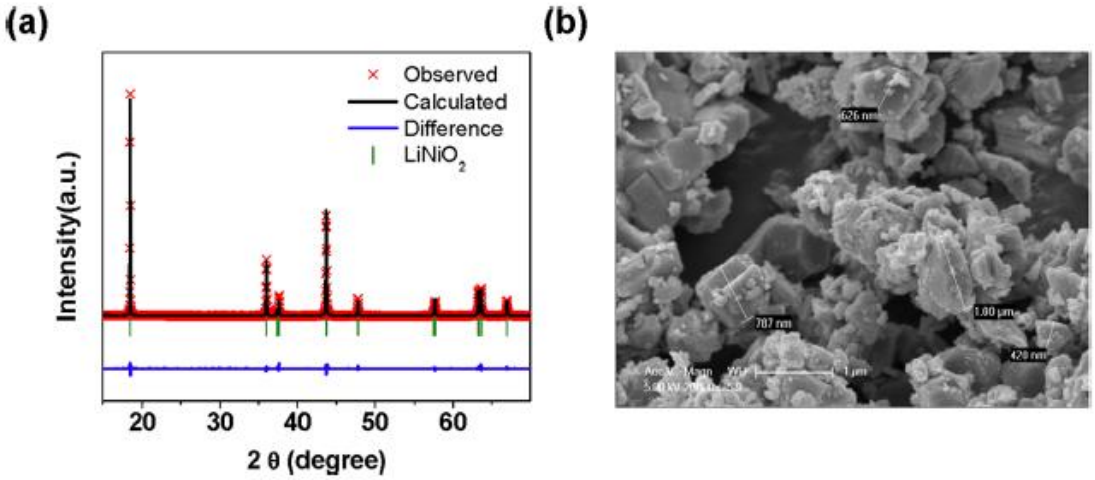

Figure 1. (a) Synchrotron high-resolution XRD pattern and refinement. (b) SEM image of the synthesized LiNiO2 sample.

In this study, we understood the factors affecting the electrochemical activity of LiNiO2, especially during the 1st cycle to determine whether the theoretical capacity of LiNiO2 can be achieved or not. Considering that there are multiple phase transformations (H1−M−H2−H3) during charge/ discharge, we investigate the effects of these structural changes on the electrochemical activity by controlling the upper cut-off voltages of LiNiO2. Especially, we focus on understanding the low Coulombic efficiency of LiNiO2. We found out that the low

CE in the 1st cycle in LiNiO2 is ascribed to the low discharge capacity that is caused by a sluggish additional discharge reaction at ∼3.5 V rather than detrimental phase transitions such as H2−H3 at ∼4.2 V, which leads to a severe volume change. The activation in this discharge reaction strongly depends on the kinetics. At low current density, the 3.5 V discharge reaction can be activated and thereby the achievable discharge capacity is increased, leading to high CE. However, this 3.5 V discharge reaction at high current density is not activated. This indicates that the kinetics of the 3.5 V discharge reaction is very slow. In the galvanostatic intermittent titration technique (GITT) measurement, the sluggish 3.5 V discharge reaction is almost fully activated, and thereby the LNO can achieve 100% CE with the 4.3 V cut-off voltage, leading to ∼250 mAh/g of discharge capacity. Furthermore, the GITT data clearly shows that the LiNiO2 has an additional electrochemical reaction at ∼3.6 V for the charge and at ∼3.5 V for the discharge. However, these additional reactions for the charge and discharge are kinetically
asymmetric; the additional discharge reaction at ∼3.5 V shows much higher polarization than the additional charge reaction at ∼3.6 V. This further confirms that the 3.5 V discharge reaction has very poor limited kinetics. Through nuclear magnetic resonance (NMR) and neutron diffraction data, we found out that the insertion of Li into the bulk at the end of the discharge at 3.5 V is not easy and can be accompanied by the rearrangement of cations such as Li and Ni or local structural changes resulting in poor kinetics. These understandings and findings will give alternative strategies for improving the electrochemical performance of Ni-rich layered materials as the Ni content increases and LiNiO2 for high energy density LIB.

2. EXPERIMENTAL SECTION

2.1. Preparation of Materials. LiNiO2 was prepared by mixing LiNO3 and Ni(OH)2 with acetone (high-performance liquid
chromatography (HPLC) grade) in a molar ratio of 1.01:1 by ballmilling for 12 h. After mixing these precursors, the mix was ball-milled using a planetary ball-milling machine for 5 h and then calcined at 750 °C for 12 h under oxygen.

2.2. Material Characterization. Synchrotron X-ray diffraction (XRD) measurement was performed on beamline 9B-HRPD at Pohang Accelerator Laboratory, Pohang, Korea. The incident X-rays were vertically collimated by a mirror and monochromated to the wavelength of 1.4970 Å using a double-crystal Si(111) monochromator. The datasets were collected in the range of $10° \leq 2\theta \leq 130°$ with a step size of 0.02° (2θ range). The lattice parameters of the samples and the quantity of impurities were determined using FullProf software.3 The neutron diffraction measurements were performed at the Australian Center for Neutron Scattering. The wavelength was 1.5340 Å, and the scan range was 10−150° in increments of 0.05. The lattice parameters of the samples and the degree of Ni/Li disordering were determined using FullProf software. The morphology of the particles was observed using a field-emission scanning electron microscope (FE-SEM, Philips electron optics B.V XL30S FEG).

2.3. Nuclear Magnetic Resonance (NMR) Measurements. 6Li NMR measurements were performed at RT using a Bruker Avance- 200 spectrometer (B0 = 4.7 T, Larmor frequency ν0 = 29.28 MHz). Magic angle spinning (MAS) spectra were obtained using a Bruker MAS probe with a cylindrical 2.5 mm (o.d.) zirconia rotor. Spectra were acquired at a spinning frequency of 34 kHz. 6Li-MAS-NMR spectra were acquired using an echo (π/2−τ−π−τ) pulse sequence with a π/2 pulse of 4.1 μs. The recycle time was typically 0.5 s. The isotropic shifts, reported in parts per million (ppm), are relative to an external liquid 1 M solution of LiCl set at 0 ppm. 6Li integrated intensities were determined using spectral simulation (Dmfit software).

2.4. Electrochemical Measurements. For the galvanostatic electrochemical test, the lithium metal half-cells were assembled using a Swagelok-type cell in a glovebox. The composite electrode with the ratio of active material 80 wt %/super-P (carbon black, Timcal) 15 wt %/binder 5 wt % (poly(tetrafluoroethylene) (PTFE)) was prepared by rolling into a thin sheet with uniform thickness and size. The active material loading was 2−4 mg/cm2. The active composite cathode and a lithium metal anode were separated by a porous polypropylene film (Celgard 2400). The electrolyte used was 1 M LiPF6 dissolved in ethylene carbonate/diethyl carbonate (EC/DEC) (1:1 by volume, PANAX ETEC Co. Ltd.) solution. All cells were operated at room temperature.

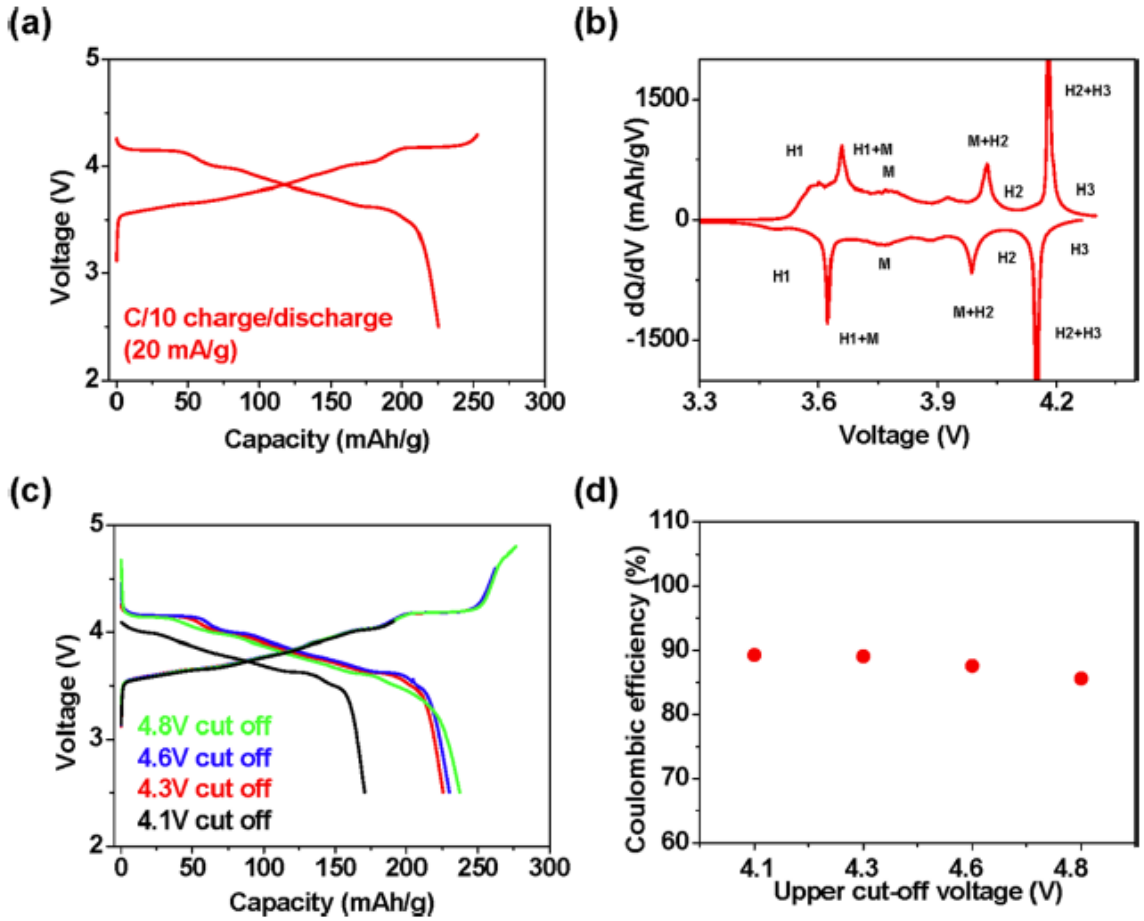

Figure 2. (a) Voltage profile of the LNO electrode at C/10 charge and C/10 discharge rates with the 4.3 V upper cut-off voltage, and (b) its differential capacity plot (dQ/dV) as a function of voltage, (c) voltage profiles of the 1st cycle of the LNO electrodes with various upper cut-off voltages (4.1, 4.3, 4.6, and 4.8 V) at C/10 charge and C/10 discharge rates and (d) their Coulombic efficiencies at the 1st cycle.

3. RESULTS

LiNiO2 (LNO) was prepared via a simple solid-state reaction under oxygen. Synchrotron XRD data in Figure 1a shows that the LNO sample has a typical rhombohedral (R) phase without any impurity phases. The lattice parameters of the synthesized LNO sample obtained from the Rietveld refinement were a = 2.87646 (1) Å and c = 14.19798 (13) Å (Table S1), which are similar to the reported values12 and the amount of Ni in the Li layer (the degree of the cation disordering) was ~1.2% (Table S2), indicating that the sample has a negligible

degree of the cation disordering.12 The SEM image in Figure 1b clearly shows that the LNO sample has ∼0.1−2 μm in size with a broad range of the size distribution and has irregular faceted morphology of particles. To understand the electrochemical activity of the LiNiO2 (LNO) sample during the 1st cycle, electrochemical tests were carried out with various upper cut-off voltages because the multiple phase transitions in a charge process occur and strongly depend on the upper cut-off voltages. In Figure 2a, the LNO sample cycled with a 4.3 V cut-off voltage shows charge/ discharge voltage curves and capacities (250 mAh/g in charge, and 225 mAh/g in discharge) that are quite similar to the previously reported results in the literature.13 Also, the differential capacity plot, dQ/dV, in Figure 2b displays the multiple phase transitions undergone by the LNO sample during charge/discharge. This is consistent with the wellknown phase transition behaviors referred to as the H1−M− H2−H3 phase transition.14 The original hexagonal structure in LiNiO2 is denoted by H1, and this H1 structure transforms into M, H2, and H3 phases during the charge. The H1 phase transforms into the M phase at ∼3.65 V in charge, and then this M phase transforms into another hexagonal phase (H2) at ∼4.05 V. At the voltage plateau at ∼4.2 V during the charge, the H2 phase gets transformed into the H3 phase via phase separation. Since the H3 phase has a much smaller c lattice parameter compared to the H2 phase, the H2−H3 phase transition can induce a substantial volume change that can easily lead to the formation of cracks on the surface of the particle. These multiple phase transitions have clear peaks in the differential capacity plot (dQ/dV) of LiNiO2 in Figure 2b.15 By decreasing the cut-off voltage from 4.3 to 4.1 V, both charge and discharge capacities were decreased and the H2− H3 phase transition, which is indicated by the plateau at ∼4.2 V, disappeared, as shown in Figure 2c. However, when the cutoff voltage increases from 4.3 to 4.6 V, the charge capacity increased to 262 from 250 mAh/g, but the discharge capacity barely increased and was similar to the obtained discharge capacity for the 4.3 V cut-off voltage in Figure 2c. The increase in the cut-off voltage from 4.3 to 4.6 V for achieving high discharge capacity is unambiguously not effective. Further increase in the cut-off voltage from 4.3 to 4.8 V also increases the charge capacity, which is similar to the theoretical capacity of LNO, but it does not increase achievable discharge capacity. After the charge ending with the 4.8 V cut-off voltage, the discharge voltage profile shows a sloping shape with large voltage polarization in Figure 2c, which is slightly different from the discharge voltage curve of the 4.3 or 4.6 V cut-off voltage. This can be caused by the bulk structural changes due to the complete phase transformation into the H3 phase when reaching 4.8 V or side reactions on the surface with the electrolyte during the charge process at high voltage.16 Also, in Figure 2c, the Coulombic efficiency of the LNO electrode at the 4.8 V cut-off voltage was lower than that at the 4.3 V cutoff voltage, indicating that its electrochemical irreversibility is increased by charging up to 4.8 V and discharging. Figure 2d shows that the 1st Coulombic efficiencies of the LNO sample with various upper cut-off voltages are not 100% but are close to 90%, irrespective of cut-off voltages. Surprisingly, the cell with the 4.1 V cut-off voltage still shows the low Coulombic efficiency at the 1st cycle even though the LNO sample does not undergo the H2−H3 phase transition at ∼4.2 V, which is known to induce severe structural changes, and even though side reactions with the electrolyte barely occur at 4.1 V. This indicates that the low 1st Coulombic efficiencies of the LNO sample are not ascribed to the structural changes caused by the H2−H3 phase transition or to the reaction on the surface with the electrolyte during charging and discharging. The charge capacity almost linearly increases with respect to the increase in the upper cut-off voltages, whereas the discharge capacity does not. This
indicates that the low 1st Coulombic efficiency behavior can be caused by a limited discharge capacity that can be caused by a limited discharge reaction rather than the multiple phase transitions such as H2−H3 occurs at 4.3 V. To further increase the discharge capacity of LiNiO2, the reason why the discharge reaction is not fully activated even at low upper cut-off

voltage needs to be understood. It should be noted that the LNO sample shows a typical capacity retention behavior at the C/ 3−C/3 rate, which is a continuous capacity decay with a continuous decrease of the degree of the H2−H3 phase transition during cycles (Figure S1).

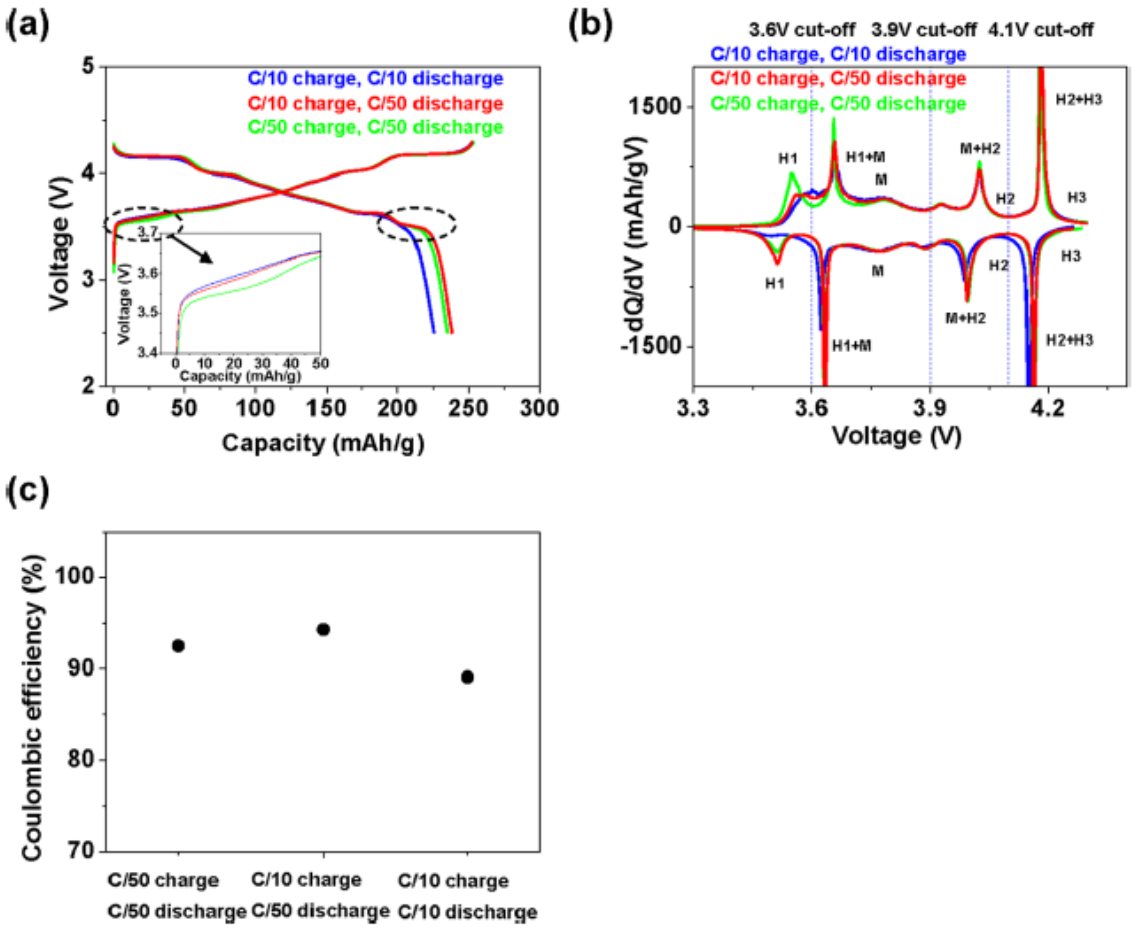

Figure 3. (a) Voltage profiles of the LNO electrodes with different charge and discharge rates (C/10, C/50). (b) Differential capacity (dQ/dV) plots of the LNO electrodes at different charge/discharge rates. (c) 1st Coulombic efficiencies at various charge and discharge rates (C/10, C/50).

To understand the limited discharge reaction in LNO materials, electrochemical tests at different discharge rates were carried out. For a discharge at the C/50 rate with the charge at the C/10 rate, the LNO sample in Figure 3a shows a distinct increase in the discharge capacity even with the same 4.3 V upper cut-off voltage. This is quite different from the discharge behavior observed for the C/10 discharge rate subsequent to the C/10 charge rate. The discharge capacity of the LNO electrode at the C/50 discharge rate increases to 236 from 225 mAh/g at the C/10 discharge rate, leading to an increase in the Coulombic efficiency. Given that the charge capacity at both C/10 and C/50 discharge rates is almost the same, this indicates that the discharge reaction in the LNO sample can be susceptible to the current density or the kinetics. The increase in the discharge capacity can be ascribed to the additional voltage plateau at ~3.5 V that is only observed in the discharge at the C/50 rate, not at the C/10 rate in Figure 3a,b. This indicates that the LNO sample has a kinetically limited

discharge reaction at ~3.5 V. When the cell was charged at the C/50 rate, as shown in Figure 3a, the polarization of the charge reaction at ~3.6 V, which can be the corresponding reaction to the discharge reaction at ~3.5 V, decreases compared to that of the charge reaction at the C/10 rate. Even though the polarization of the charge reaction at ~3.6 V is lowered at the C/50 charge rate, the charge capacity in the charge at the C/50 rate barely increases compared to that at the C/10 charge rate. This indicates that the charge reaction at ~3.6 V seems to be activated even at the C/10 charge rate even with a slight increase in the polarization unlike the 3.5 V discharge reaction, which is barely activated at the C/10 discharge rate. Figure 3b shows the differential capacity (dQ/dV) plots of the LNO sample at different charge/discharge rates. The differential capacity plots clearly show that a peak at ~3.5 V in the discharge reaction is observed only at the C/50 discharge rate. This indicates that the additional discharge reaction at ~3.5 V is kinetically very slow and its activation at very low current density can increase the discharge capacity. The cell with the C/50 charge−C/50 discharge rate clearly shows a peak at ~3.6 V in the charge and the corresponding peak at ~3.5 V in the discharge. This indicates that the LNO sample has an additional electrochemical reaction at ~3.6 V for the charge and ~3.5 V for the discharge. As a result, the Coulombic efficiency of the cells with C/50 discharge rates can increase to 95 from 90% at the C/10 discharge rate. Given that the H1 phase is related to both the additional discharge reaction at ~3.5 V and the charge reaction at ~3.6 V, the insertion of Li into the H1 phase at the end of the discharge is kinetically much harder than the extraction of Li from the H1 phase at the beginning of the charge. This asymmetric reaction of the H1 phase during the charge and discharge behavior is similar to the reported result in high Ni NMC materials.17 In LNO materials, the sluggish discharge reaction at ~3.5 V can cause a limited achievable discharge capacity, whereas the corresponding charge reaction at ~3.6 V is not kinetically limited, leading to low Coulombic efficiency at the 1st cycle. Also, it was confirmed that the 3.5 V discharge reaction observed at the C/ 50 discharge rate at the 1st cycle is still active in the 2nd cycle when the discharge rate was C/50 (Figure S2). In Figure S2a, it is clear that the activation of the 3.5 V discharge reaction at the C/50 discharge rate can increase not only the 1st discharge capacity but also the 2nd discharge capacity compared to that at the C/10 charge−C/10 discharge for 2 cycles, as shown in Figure S2b. To further increase the achievable discharge capacity even with low cut-off voltage, the sluggish 3.5 V discharge reaction should be understood and fully activated.

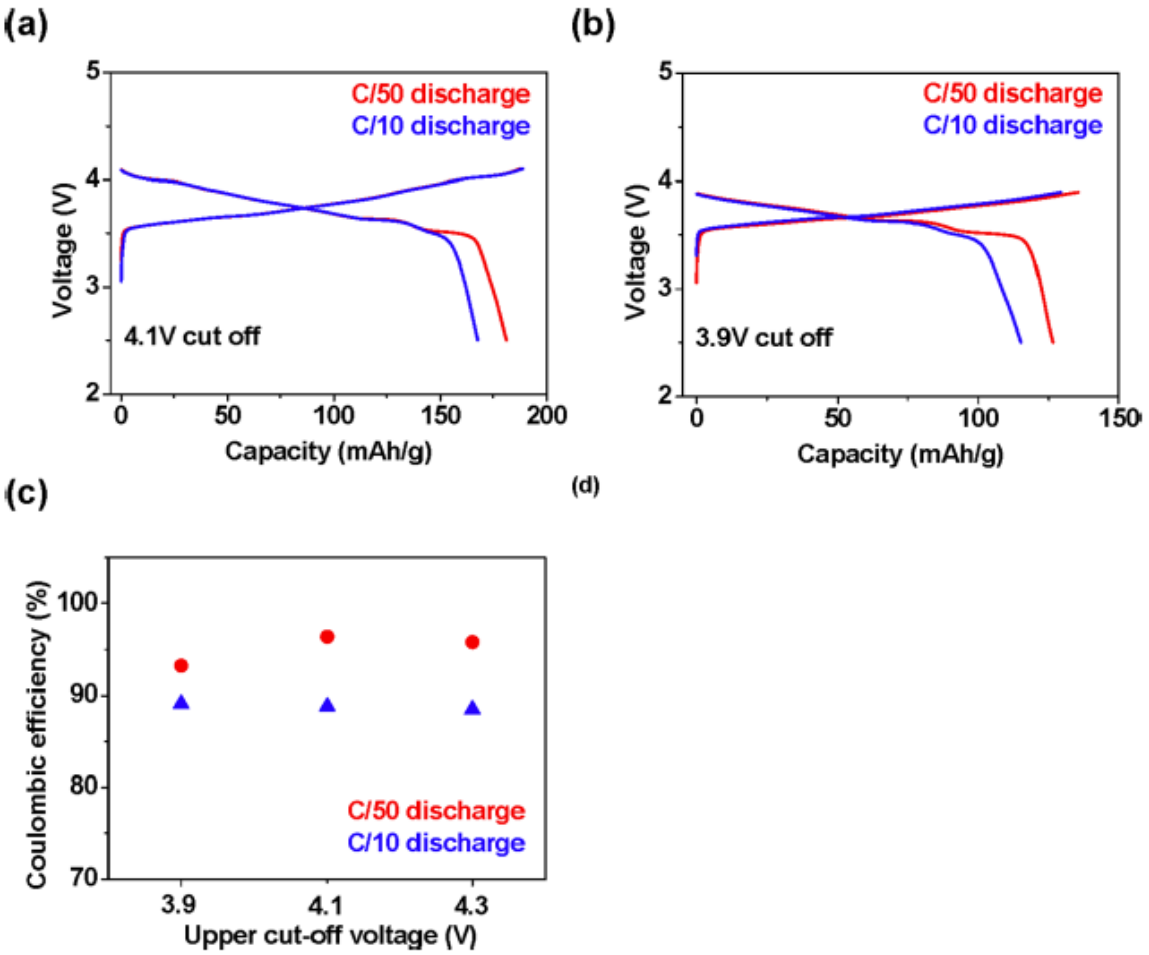

Figure 4. Voltage profiles of the LNO electrodes at the C/10 discharge rate and the C/50 discharge rate with (a) 4.1 V cut-off voltage, (b) 3.9 V cut-off voltage, and (c) 1st Coulombic efficiencies at various upper cut-off voltages with different current rates. The charge rate was C/10 for all electrodes.

To understand the effect of the phase transition behaviors, which induce structural changes, on the achievable discharge capacity, especially on the 3.5 V discharge reaction, electrochemical tests at different discharge rates with different upper cut-off voltages, as shown in Figure 3b, were carried out. The charge rate for cell tests was fixed at the C/10 rate because the achievable charge capacity barely depends on the current density. The upper cut-off voltages were decreased from 4.3 to 4.1 and to 3.9 V. It should be noted that the upper cut-off voltages were chosen by the phase transition behavior as shown in Figure 3b. The discharge capacities at the C/50 discharge rate increase irrespective of the cut-off voltages compared to those at the C/10 discharge rate because the 3.5 V discharge reaction is always activated at the C/50 discharge rate. This indicates that the activation of the 3.5 V discharge reaction strongly depends on the current density rather than the phase transformation behaviors. Moreover, as seen in Figure 4a, the discharge capacity also increased for a C/50 discharge rate with the 4.1 V cut-off voltage, without undergoing the H2−H3 phase transition during the previouscharge. This indicates that the increase in the discharge capacity is barely affected by the H2−H3 phase transition at ~4.2 V. In the case of a 3.9 V cut-off voltage, where the M−H2 phase transition does not occur, the discharge capacity at the C/50 discharge rate, as shown in Figure 4b, is still higher than that at the C/10 discharge rate, indicating that

the increase in the discharge capacity barely depends on the M−H2 phase transition. Further decrease of the cut-off voltage similarly leads to an increase in the discharge capacity at the C/50 discharge rate. For all upper cut-off voltages, the increase in the discharge capacity at the C/50 discharge rate is ascribed to theadditional voltage plateau at ~3.5 V in the discharge. As a result, 1st Coulombic efficiencies at the C/50 discharge rate in spite of different upper cut-off voltages are always higher than those of the C/10 discharge rate, as shown in Figure 4c. To understand the electrochemical properties of the 3.5 V discharge reaction, galvanostatic intermittent titration technique (GITT) tests at 4.3 V cut-off voltages were carried out. The cells were charged/discharged for 1 h at the C/100 rate (2 mA/g) at each step and rested for 2 h at each step. Surprisingly, the 1st Coulombic efficiency of LiNiO2 in the GITT test is almost 100% with the 4.3 V cut-off voltage in Figure 5a, indicating that the fully reversible delithiation/ lithiation of the LiNiO2 material is possible. In the GITT voltage profile in Figure 5a, the LNO sample shows an additional voltage plateau at the beginning of the charge and at the end of the discharge, where the electrochemical reaction is mainly related to the H1 phase and determines the achievable discharge capacity. The differential capacity plot of the OCV also shows an additional peak at ~3.6 V for the charge and ~3.5 V for the discharge (dotted box in Figure 5b). This is consistent with the electrochemical behavior at the C/50 charge−C/50 discharge rate (Figure 3a,b). This clearly demonstrates that the LNO sample has an additional electrochemical reaction in both charge and discharge but this reaction can be strongly susceptible to the kinetics or current density. Given that this electrochemical reaction has a flat voltage behavior in the H1 phase region in the GITT test, a phase separation reaction at this region can be undergone via forming a new phase. Unfortunately, the new phase in this region, especially for the discharge reaction was not observed in synchrotron XRD measurement in Figure S3. This can be due to the fact that the new phase can be structurally quite similar to the H1 phase. Furthermore, the additional electrochemical reaction in the H1 phase region shows a quite different polarization behavior compared to other electrochemical reactions at higher potential regions even though the applied current density is very low. In Figure 5c, the LNO sample shows almost negligible polarization in most of the charge and discharge reactions, except for the beginning of the charge and the end of the discharge, where the additional electrochemical reaction occurs. This indicates that the insertion (extraction) of Li into (from) the H1 phase is not facile compared to other phases during charge/discharge. However, the polarization of the discharge reaction at ~3.5 V is much higher in a wide composition range than that of the charge reaction. This indicates that the insertion of Li into the H1 phase at the end of the discharge is kinetically very sluggish compared to the extraction of Li from the H1 phase at the beginning of the charge. The very beginning of the charge (<10 mAh/g) in Figure 5c shows the polarization of ~<0.15 V but the rest of the charge shows very low polarization, indicating that the kinetics does not critically affect the charge reaction. In contrast, the discharge reaction in the H1 phase region shows a very high polarization of >0.2 V even with very low current density in a wide composition range from the composition where the 3.5 V discharge reaction (<50 mAh/g) starts to the end of the discharge. This indicates that the discharge reaction at ~3.5 V is kinetically very limited. As a result, the CE in the 1st cycle strongly depends on the activation of the 3.5 V discharge reaction.

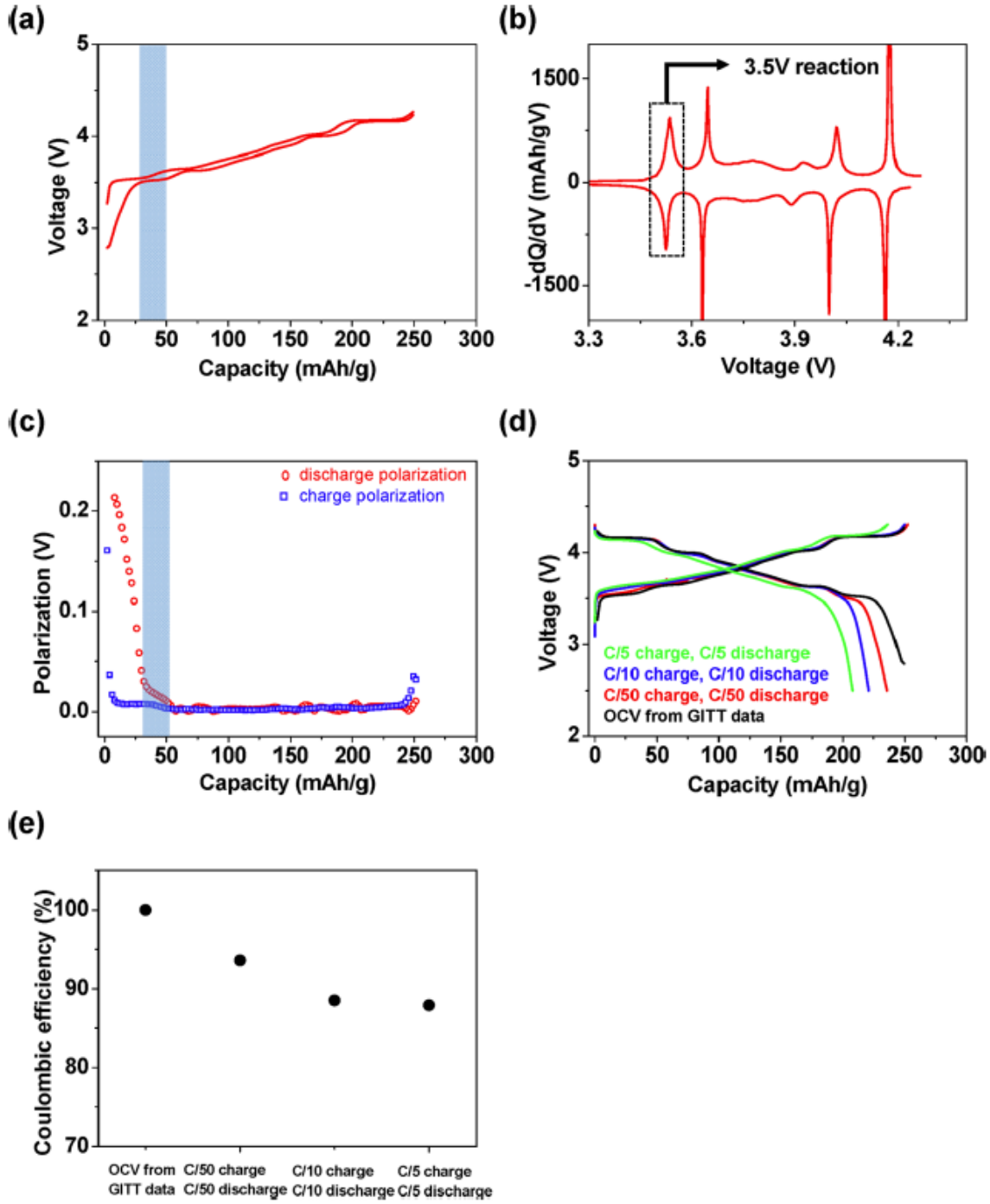

Figure 5. (a) Open-circuit voltage (OCV) of the LNO electrode obtained with the GITT test, (b) differential capacity plot with respect to the OCV in the LNO electrode, (c) the polarization curve obtained from GITT measurement with the 4.3 V cut-off voltage, (d) voltage profiles of LNO electrodes at various charge and discharge rates, and (e) 1st Coulombic efficiencies of LNO cathodes at various charge and discharge rates.

Figure 5d,e shows the voltage curves of LiNiO2 and initial Coulombic efficiencies at various charge rates and discharge rates with the 4.3 V cut-off voltage, respectively. The charge capacity at the C/10 rate is a little higher than that at the C/5 charge rate, but the charge

capacity at the C/50 rate does not further increase compared to that at the C/10 rate charge. The voltage profiles of the charge at different rates are almost similar, except at the beginning of the charge.

At the C/50 charge rate, the voltage profile at the beginning of the charge shows slightly lower polarization than at the C/10 rate. This indicates that the extraction of Li in the H1 phase is slightly affected by the current density but the obtained charge capacity is not. However, the discharge capacities of the LNO electrodes are linearly increased by slowing discharge rates or current densities (C/5−C/10−C/50−C/100 (GITT)). The increase in the discharge capacity with the current density is caused by the additional discharge voltage plateau at ~3.5 V, which is observed only at C/50 and GITT. This indicates that the activation of the 3.5 V discharge reaction critically depends on the kinetics. In LNO material, the additional electrochemical reaction at ~3.5 V is observed but is not kinetically symmetric in the charge/discharge because of the kinetically limited discharge reaction at ~3.5 V. As a result, the discharge capacity is not fully achieved even at a reasonable low current density (<C/10 discharge rate) making 100% CE in the 1st cycle very difficult.

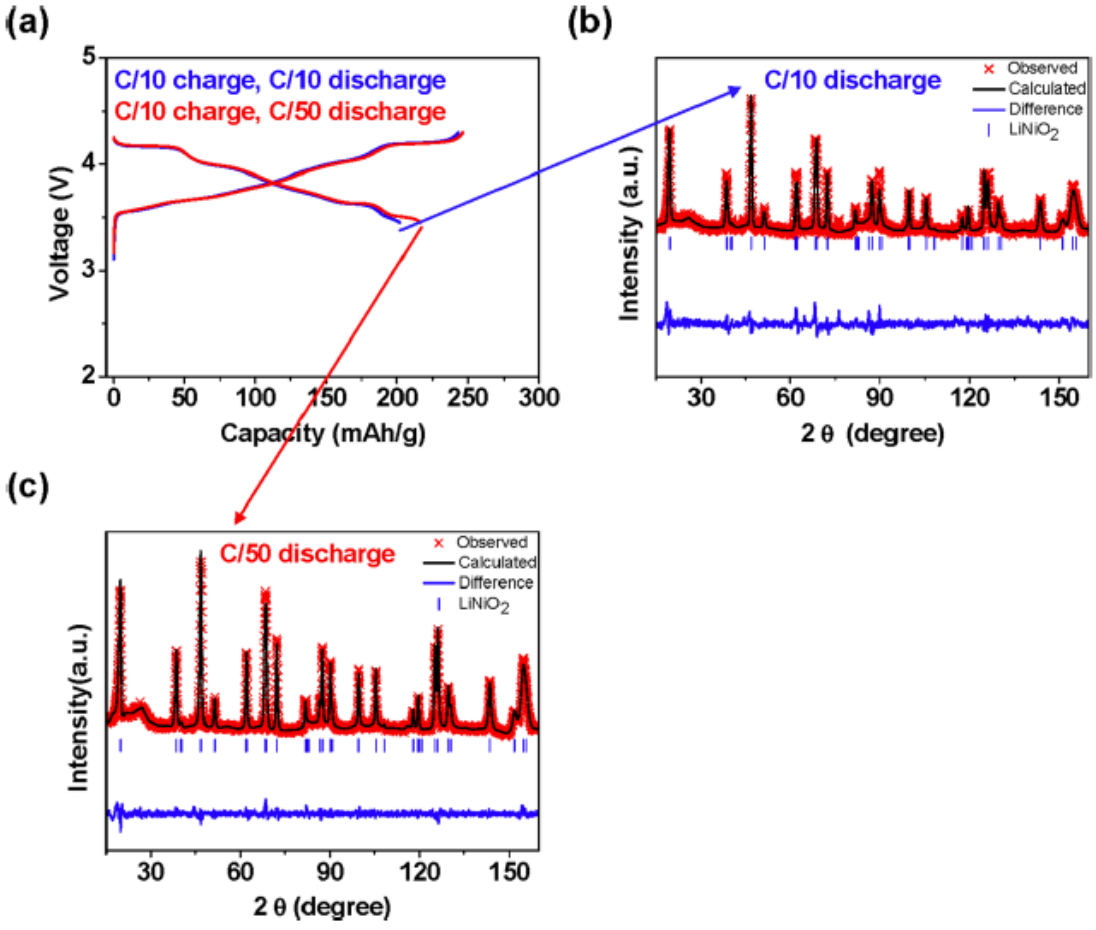

Figure 6. (a) Voltage profiles of the two electrodes with different discharge rates, C/10 and C/50 with the 3.45 V discharge cut-off voltage. Neutron diffraction patterns of the LNO electrode with the 3.45 V discharge cut-off voltage at (b) the C/10 discharge rate, and (c) the C/50 discharge rate.

Table 1. Lattice Parameters and the Amount of Li and Ni in the Pristine LiNiO2, the C/10 Discharged Electrode, and the C/50 Discharged Electrode with the 3.45 V Cut-Off Voltage[a]

refined parameters		sample name		
		pristine	C/10	C/50
$LiNiO_2$ (R-3m)	a	2.87344(4)	2.87110(9)	2.87304(6)
	c	14.18222(37)	14.21287(75)	14.20084(34)
atom occupancies (Li/Ni)	Li layer (3a)	0.988(1)/0.012(1)	0.782(2)/0.027(2)	0.861(1)/0.005(1)
	TM layer (3b)	0.012(1)/0.988(1)	0.027(2)/0.973(2)	0.005(1)/0.995(1)

[a]Overall Li/Ni occupancies: (0.809, 1) in C/10, (0.866, 1) in C/50.

To understand the structural changes such as the Li/Ni disordering caused by the activation of the sluggish 3.5 V discharge reaction, ex situ neutron diffraction measurements in the two electrodes were carried out and the change in the Li/ Ni disordering depending on the activation of the additional 3.5 V discharge reaction in the sample was carefully measured. The two electrodes were prepared with different discharge rates: one electrode was undergone by the 3.5 V discharge reaction and the other electrode was not. The electrodes were charged to 4.3 V at the C/10 rate and discharged to 3.45 V in different discharge rates, C/10 and C/50 rates in Figure 6a. The discharge curve at the C/50 discharge rate clearly shows additional voltage plateau but that at the C/10 discharge rate does not. The discharge capacity at the C/50 discharge rate is higher by ∼10 mAh/g than the discharge capacity at a C/10 discharge rate. This indicates that the sluggish ∼3.5 V discharge reaction is activated at the C/50 discharge rate, not at the C/10 discharge rate. Based on the neutron diffraction data, the two electrodes show similar structural characteristics; the lattice parameters of the two electrodes obtained from Rietveld refinement results in Table 1 are similar to each other; a = 2.87110(9) Å, c = 14.21287(75) Å for the C/10 discharged electrode and a = 2.87291(6) Å, c = 14.19953(51) Å for the C/50 discharged electrode. The ex situ synchrotron XRD measurements show negligible structural changes of the two electrodes during the 3.5 V discharge reaction in LiNiO2 (Figure S3), and this is consistent with previous work by Li et al.18 However, the refinement results of the neutron diffraction data in Table 1 shows that the C/50 discharged electrode has a slightly different degree of Li/Ni disordering (intermixing) compared to the C/10 discharged electrode and the pristine material (Table S2). The degree of Li/Ni disordering in the C/50 discharged electrode substantially decreased to 0.5% from that (2.7%) of the C/10 discharged electrode and is slightly lower than that of pristine LNO (1.2%), whereas the degree of Li/Ni disordering (2.7%) of the C/10 discharged electrode is higher than that of pristine LNO (1.2%). Considering that the charge/discharge voltage curve of the electrode with the C/50 discharge rate is almost identical to that of the electrode with the C/10 discharge rate before the 3.5 V discharge reaction, the lowering of Li/Ni in the C/50 discharged electrode can be caused by the additional voltage plateau at 3.5 V. As a result, the increase in the discharge capacity in the C/50 discharged electrode can be correlated to the decrease in the Li/Ni disordering. This indicates that the further insertion of Li into the LNO in the C/50 discharge rate by activating the 3.5 V discharge reaction can go to the Li layers and thereby can cause the rearrangement of Ni ions, which already exist in the Li layer due to the increase in the Li/Ni disordering, leading to a decrease in the Li/Ni disordering. As a result, the kinetically limited reaction at the 3.5 V discharge reaction can be ascribed to the fact that the Li insertion can be accompanied by the local structure changes via the rearrangement of cations, which can induce high voltage polarization.

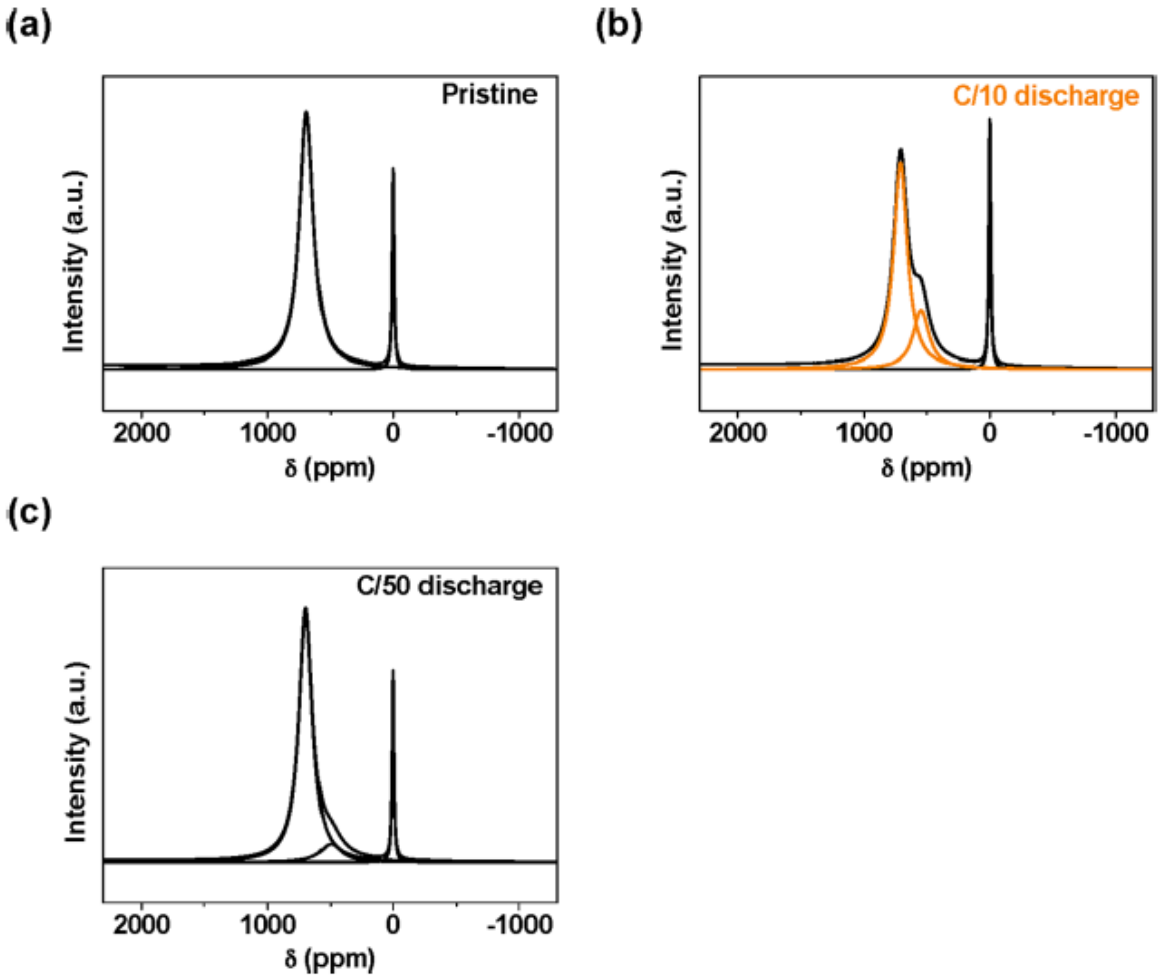

Figure 7. Normalized 6Li-MAS-NMR calculated spectra of the electrodes: (a) the pristine LiNiO2 electrode, (b) the C/10 discharged electrode with the 3.45 V cut-off voltage, and (c) the C/50 discharged electrode with the 3.45 V cut-off voltage.

To understand the change in the local Li environment, which is induced by the additional discharge voltage plateau at ∼3.5 V, 6Li magic angle spinning−nuclear magnetic resonance (6Li-MAS-NMR) measurements were carried out (Figure 7). In the pristine LNO sample, two types of local environments of Li can be distinguished; one major contribution at 690 ppm, which can be assigned to Li in the Li layer of LiNiO2,19 and a sharp peak at 0 ppm coming most likely from Li2CO3 on the surface even though the XRD measurement does not show the Li2CO3 impurity phase. The contamination of Li2CO3 on the surface is typically observed in Ni-rich layered materials.20 Considering that the NMR experiments in the present study have been performed at 34 kHz, the observed 6Li shift at 690 ppm is in good agreement with the lower expected shift for a stoichiometric LiNiO2 compared to previous works by Chazel et al.19 and Carlier et al.,21 showing higher experimental 6Li and 7Li hyperfine shifts for Li in the Li layer of LiNiO2 at 750 and 714 ppm, respectively. The normalized spectrum of the C/ 50 discharged electrode also displays a major resonance at ∼694 ppm, which is very

similar to that for the pristine sample. This indicates that the Li local environments in LNO after a discharge at C/50 are similar to that of the pristine LNO. This result suggests that Li local environments in $LiNiO_2$ are barely modified after a charge followed by a slow C/50 discharge. On the contrary, the normalized spectra of the C/10 discharged electrode with the 3.45 V cut-off voltage display a major resonance at ~710 ppm. While this shift is consistent with the density functional theory (DFT) predictions22 for Li local environments in $LiNiO_2$, supporting its attribution to Li in Li layers, it appears at a significantly higher shift compared to that for the pristine and the C/50 sample, highlighting the differences in local Li environments in the two electrodes. Considering that the Ni^{3+} ions have a noncooperative Jahn−Teller effect,13,22 which is related to the local distortion of NiO_6 octahedra and thereby can lead to a hyperfine shift, it seems reasonable to assert that additional local distortions can cause further shifts in the case of the sample discharged at the C/10 rate compared to the C/50 rate discharged electrode. One possibility is that the Li/Ni disordering could cause this kind of distortion. Although it is difficult to determine experimentally and would require calculations, it is interesting to note that the LNO sample discharged at C/10 exhibits a significant Li/Ni disordering, 2.7% from neutron diffraction refinements, compared to the pristine (1.2%) and the sample discharged at C/50 (0.5%), suggesting that there may be a link between the Li/Ni disordering and the distortions of the Li and Ni local environments responsible for the higher hyperfine shift observed for the sample discharged at C/10. The two electrodes operated at different discharge rates show an additional resonance in the 490−550 ppm range (Table 2). These two resonances account for 25 and 15% of the total integrated intensity (leaving out the Li_2CO_3 contribution) for the sample discharged at C/10 and C/50, respectively. This is in good agreement with the refined overall Li/Ni occupancies: 0.809 after a discharge at C/10 and 0.866 after a discharge at C/50, suggesting that close to 19 and 13% Ni^{4+} exist due to not fully inserted Li ions at the two electrodes. These results suggest that the additional resonances observed in the 490−500 ppm range are related to the presence of remaining Ni^{4+} nearby Li in the layered structure in the electrode.23 Higher percentages that can be obtained from NMR data are probably due to the fact that one remaining Ni^{4+} could be “seen” by more than one Li^+ ion in its vicinity, leading to an overestimation of the corresponding local environments by NMR. It is difficult to determine whether the discrepancy between the experimentally observed additional resonances at 543 ppm for the discharged at C/10 and 494 ppm for the discharged at C/50 is due to additional structural distortions modifying the magnitude of the hyperfine shifts or not. Also, the C/50 discharged electrode shows a much broader FWHM of the resonance at ~543 ppm than that of the C/10 discharged electrode shown in Table 2. This indicates that the Li local environments nearby Ni^{4+} ions in the C/50 discharged electrode are more distributed compared to the C/10 discharged electrode. The local distortions in the C/50 discharged electrode might lead to the broad distribution of Li. These results indicate that the increase in the discharge capacity at C/50 compared to the C/10 rate can originate clearly from Li insertion in Li layers as shown by the NMR measurements. Structure refinements also show that the LNO electrode presents different degrees of Ni disordering at the end of the discharge that may be seen indirectly by NMR as an additional hyperfine shift induced by local distortions. As the insertion of Li at the end of the discharge is more difficult to progress upon the C/10 discharge rate, it shows that Li rearrangement in the Li/Ni layer in the layered structure can be correlated to the activation of the 3.5 V discharge reaction, which is in good agreement with the ex situ neutron diffraction data.

Table 2. Main Peak Position and Its Full Width at Half- Maximum (FWHM) of the 4.3−3.45 V Ex Situ Electrodes in C/10 and C/50 Discharged and Pristine Electrodes

	pristine	C/10	C/50
main peak (ppm)	688.20	708.42	693.98
FWHM (main peak)	132.85	132.85	127.07
additional peak (ppm)		543.80	494.71
FWHM (additional peak)		155.95	207.93

4. DISCUSSION

In LiNiO2, the charge capacity increases as the cut-off voltage increases from 4.1 to 4.8 V but the discharge capacity does not. In other words, the achieved discharge capacity does not linearly increase with the increase in the charge capacity, leading to low Coulombic efficiency at the 1st cycle. The limited discharge capacity is not related to the multiple phase transition behaviors during charge/discharge (H1−M−H2− H3), especially the H2 H3 phase transition that easily causes severe structural change. However, we clearly demonstrate that the additional electrochemical reaction at ∼3.5 V can be an origin of the low Coulombic efficiency in LNO because it critically depends on the applied current density or kinetics. As a result, the additional discharge reaction at 3.5 V is barely activated at a relatively low current density (∼C/10 rate), leading to low discharge capacity of LiNiO2 and low CE at the 1st cycle. This behavior is similar to the electrochemical properties of Ni-rich layered materials (Ni > 0.8). Ni-rich layered materials also show low CE efficiency at the 1st cycle. Recently, several studies report that low Coulombic efficiency of Ni-rich layered materials can be caused by poor kinetics of Li ions,10,11,24 or the low Li diffusion kinetics in the H1 phase17 This observation is in accordance with our results in LiNiO2, indicating that the electrochemical properties of the Ni-rich layered materials can be dominated from those of LiNiO2. In addition, our results show that the sluggish reaction at the end of the discharge is barely affected by multiple phase transformations during the charge/discharge of LiNiO2. The sluggish 3.5 V discharge reaction should be well understood and must be activated to increase the discharge capacity of LiNiO2. To understand this reaction, the GITT measurement was performed. Based on GITT measurements, the LiNiO2 material can achieve 100% CE with ∼250 mAh/g of discharge capacity even with the 4.3 V cut-off voltage. Furthermore, the additional electrochemical reaction occurs in both charge and discharge and shows a voltage plateau at ∼3.6 V for the charge and ∼3.5 V for the discharge. This indicates that the insertion and the extraction of Li can be undergone by the phase separation behavior. However, the charge and discharge reactions are kinetically asymmetric; the charge reaction at ∼3.6 V can be activated but the discharge reaction at ∼3.5 V is not activated at relatively low current density (>C/10 rate). The charge reaction shows high polarization compared to other electrochemical reactions but still can be activated contributing to the achievable charge capacity. In contrast, the discharge reaction at ∼3.5 V shows much higher polarization than

the charge reaction and thereby is not easily activated, leading to low discharge capacity. Through this, the insertion of Li into the H1 phase at the end of the discharge is very difficult compared to the extraction of Li from the H1 phase at the beginning of the charge in LiNiO2. Using the NPD and Li NMR results, we clearly demonstrate that the sluggish 3.5 V discharge reaction can be correlated to the rearrangement of the cations or local structure change. In the NPD result, the activation of the sluggish 3.5 V discharge reaction in the C/50 discharged electrode lowers the degree of the cation disordering compared to the C/10 discharged electrode, which has higher Li/Ni disordering (intermixing) than the pristine LiNiO2. This indicates that the sluggish 3.5 V discharge reaction can be associated with the insertion of Li in the Li layer where Ni can be already present due to a local structure change, which can be caused by the migration of Ni into Li layers within the bulk structure. With 6Li-MAS-NMR data, Li environments in the LiNiO2 bulk structure vary depending on discharge rates (C/10, C/50). When the sluggish 3.5 V discharge reaction is activated at the C/50 discharge rate, Li corresponding to the additional discharge capacity can go to Li layers and only a very small amount of remaining Ni4+ is detected. As a result, the coupling of Li insertion with local structure change at the end of the discharge at ∼3.5 V makes this discharge reaction sluggish.

5. CONCLUSIONS

In this study, the electrochemical activity, especially the Coulombic efficiency (CE), of LiNiO2 is understood to further increase the achievable discharge capacity. By electrochemical tests with different upper cut-off voltages, we found out that the 1st Coulombic efficiency of LiNiO2 is low (under 90%), irrespective of the upper cut-off voltages. Achieving theoretical charge capacity (∼275 mAh/g) was possible by increasing the upper cut-off voltage to 4.8 V, but still full discharge capacity was not achievable. Given that different upper cut-off voltages indicate different phase transformation behaviors, we show that the multiple phase transformations in LiNiO2 barely affect this low 1st Coulombic efficiency. The GITT measurement shows that the LiNiO2 material has the additional electrochemical reaction at ∼3.6 V for the charge and at ∼3.5 V for the discharge but the discharge reaction is kinetically limited. As a result, the additional ∼3.5 V discharge reaction is not easily activated, leading to low achievable discharge capacity that can cause the low 1st Coulombic efficiency. The activation of the 3.5 V discharge reaction only occurs at low current density, leading to an additional capacity of LiNiO2 in the discharge process. When the sluggish 3.5 V discharge reaction is almost fully activated with the GITT method, the LiNiO2 material can achieve ∼100% CE with ∼250 mAh/g of discharge capacity even with the 4.3 V cut-off voltage. Ex situ NPD and NMR measurements show that the sluggish 3.5 V discharge reaction is correlated to the local structural rearrangement of Li/Ni induced by further Li insertion at the end of the discharge, especially more Li takes Li layer sites where Ni is already occupied in LiNiO2 during the C/50 discharge. For achieving higher discharge capacity in LiNiO2 and other Ni-rich cathode material, the sluggish 3.5 V discharge reaction should be fully activated. The understanding and findings will open an alternative strategy to increase the achievable discharge capacity for the high-performance Li-ion batteries as the Ni amount in Ni-rich layered materials increases.

ASSOCIATED CONTENT

* Supporting Information

The Supporting Information is available free of charge at https://pubs.acs.org/doi/10.1021/acsami.1c04359.
Voltage profiles; HRPD patterns; and Rietveld refinement results of HRPD and NPD measurements (PDF)

AUTHOR INFORMATION

Corresponding Author
Byoungwoo Kang − Department of Materials Science and Engineering, Pohang University of Science and Technology (POSTECH), Pohang 37673, Republic of Korea;
orcid.org/0000-0002-8081-1908; Email: bwkang@
postech.ac.kr
Authors
Changgeun Bae − Department of Materials Science and Engineering, Pohang University of Science and Technology (POSTECH), Pohang 37673, Republic of Korea;
orcid.org/0000-0001-5622-1863
Nicolas Dupre − Institut des Materiaux Jean Rouxel (IMN), Université de Nantes, CNRS UMR 6502, Nantes Cedex 3 44322, France; orcid.org/0000-0002-0687-9357
Complete contact information is available at:
https://pubs.acs.org/10.1021/acsami.1c04359

Notes
The authors declare no competing financial interest.

ACKNOWLEDGMENTS
The authors gratefully appreciate the help from Dr. Maxim Avdeev in the neutron powder diffraction (NPD) measurement. This research was supported by the Brain Korea 21 PLUS Project for the Center for Creative Industrial Materials (F14SN02D1707). This research was supported by the Basic Science Research Program through the National Research Foundation of Korea (NRF) funded by the Ministry of Science, ICT & Future Planning (NRF-2019R1A2C2007933).

REFERENCES
(1) Ohzuku, T.; Ueda, A. Solid-State Redox Reactions of LiCoO2(R(3)M) for 4 Volt Secondary Lithium Cells. J. Electrochem. Soc. 1994, 141, 2972−2977.
(2) Zhang, X. D.; Shi, J. L.; Liang, J. Y.; Yin, Y. X.; Zhang, J. N.; Yu, X. Q.; Guo, Y. G. Suppressing Surface Lattice Oxygen Release of Li- Rich Cathode Materials via Heterostructured Spinel Li4Mn5O12 Coating. Adv. Mater. 2018, 30, No. 1801751.
(3) Shi, J. L.; Xiao, D. D.; Zhang, X. D.; Yin, Y. X.; Guo, Y. G.; Gu, L.; Wan, L. J. Improving the structural stability of Li-rich cathode materials via reservation of cations in the Li-slab for Li-ion batteries. Nano Res. 2017, 10, 4201−4209.
(4) Noh, H. J.; Youn, S.; Yoon, C. S.; Sun, Y. K. Comparison of the structural and electrochemical properties of layered Li[NixCoyMnz]O2 (x = 1/3, 0.5, 0.6, 0.7, 0.8 and 0.85) cathode material for lithium-ion batteries. J. Power Sources 2013, 233, 121−130.
(5) Ryu, H. H.; Park, K. J.; Yoon, C. S.; Sun, Y. K. Capacity Fading of Ni-Rich Li[NixCoyMn1‑ x‑ y]O2 (0.6 < = x < = 0.95) Cathodes for High-Energy-Density Lithium-Ion Batteries: Bulk or Surface Degradation? Chem. Mater. 2018, 30, 1155−1163.
(6) Bang, H. J.; Joachin, H.; Yang, H.; Amine, K.; Prakash, J. Contribution of the structural changes of LiNi0.8Co0.15Al0.05O2
cathodes on the exothermic reactions in Li-ion cells. J. Electrochem. Soc. 2006, 153, A731−A737.
(7) Dokko, K.; Nishizawa, M.; Horikoshi, S.; Itoh, T.; Mohamedi, M.; Uchida, I. In situ observation of LiNiO2 single-particle fracture during Li-ion extraction and insertion. Electrochem. Solid-State Lett. 2000, 3, 125−127.
(8) Kim, J.; Lee, J.; Bae, C.; Kang, B. Sublimation-Induced Gas- Reacting Process for High-Energy-Density Ni-Rich Electrode Materials. ACS Appl. Mater. Interfaces 2020, 12, 11745−11752.
(9) de Biasi, L.; Schiele, A.; Roca-Ayats, M.; Garcia, G.; Brezesinski, T.; Hartmann, P.; Janek, J. Phase Transformation Behavior and Stability of LiNiO2 Cathode Material for Li-Ion

Batteries Obtained from InSitu Gas Analysis and Operando X-Ray Diffraction. ChemSusChem 2019, 12, 2240−2250.
(10) Zhou, H.; Xin, F. X.; Pei, B.; Whittingham, M. S. What Limits the Capacity of Layered Oxide Cathodes in Lithium Batteries? ACS Energy Lett. 2019, 4, 1902−1906.
(11) Kasnatscheew, J.; Evertz, M.; Streipert, B.; Wagner, R.; Klopsch, R.; Vortmann, B.; Hahn, H.; Nowak, S.; Amereller, M.; Gentschev, A. C.; Lamp, P.; Winter, M. The truth about the 1st cycle Coulombic efficiency of LiNi1/3Co1/3Mn1/3O2 (NCM) cathodes. Phys. Chem. Chem. Phys. 2016, 18, 3956−3965.
(12) Xu, J.; Lin, F.; Nordlund, D.; Crumlin, E. J.; Wang, F.; Bai, J. M.; Doeff, M. M.; Tong, W. Elucidation of the surface characteristics and electrochemistry of high-performance LiNiO2. Chem. Commun. 2016, 52, 4239−4242.
(13) Xu, J.; Hu, E. Y.; Nordlund, D.; Mehta, A.; Ehrlich, S. N.; Yang, X. Q.; Tong, W. Understanding the Degradation Mechanism of Lithium Nickel Oxide Cathodes for Li-Ion Batteries. ACS Appl. Mater. Interfaces 2016, 8, 31677−31683.
(14) Yoon, C. S.; Jun, D. W.; Myung, S. T.; Sun, Y. K. Structural Stability of LiNiO2 Cycled above 4.2 V. ACS Energy Lett. 2017, 2, 1150−1155.
(15) Li, W.; Reimers, J. N.; Dahn, J. R. In-Situ X-Ray-Diffraction and Electrochemical Studies of Li1‑ XNiO2. Solid State Ionics 1993, 67, 123−130.
(16) Croguennec, L.; Pouillerie, C.; Delmas, C. Structural characterisation of new metastable NiO2 phases. Solid State Ionics
2000, 135, 259−266.
(17) Hong, C. Y.; Leng, Q. Y.; Zhu, J. P.; Zheng, S. Y.; He, H. J.; Li, Y. X.; Liu, R.; Wan, J. J.; Yang, Y. Revealing the correlation between structural evolution and Li+ diffusion kinetics of nickel-rich cathode materials in Li-ion batteries. J. Mater. Chem. A 2020, 8, 8540−8547.
(18) Li, H. Y.; Zhang, N.; Li, J.; Dahn, J. R. Updating the Structure and Electrochemistry of LixNiO2 for 0 < = x < = 1. J. Electrochem. Soc. 2018, 165, A2985−A2993.
(19) Chazel, C.; Menetrier, M.; Croguennec, L.; Delmas, C. 6/7Li NMR study of the Li1‑ zNi1+zO2 phases. Magn. Reson. Chem. 2005, 43, 849−857.
(20) Xiao, J.; Hu, J. Z.; Wang, D. Y.; Hu, D. H.; Xu, W.; Graff, G. L.; Nie, Z. M.; Liu, J.; Zhang, J. G. Investigation of the rechargeability of LiO2 batteries in non-aqueous electrolyte. J. Power Sources 2011, 196, 5674−5678.
(21) Carlier, D.; Menetrier, M.; Grey, C. P.; Delmas, C.; Ceder, G. Understanding the NMR shifts in paramagnetic transition metal oxides using density functional theory calculations. Phys. Rev. B 2003, 67, No. 174103.
(22) Middlemiss, D. S.; Ilott, A. J.; Clement, R. J.; Strobridge, F. C.; Grey, C. P. Density Functional Theory-Based Bond Pathway Decompositions of Hyperfine Shifts: Equipping Solid-State NMR to Characterize Atomic Environments in Paramagnetic Materials. Chem. Mater. 2013, 25, 1723−1734.
(23) Shimoda, K.; Murakami, M.; Komatsu, H.; Arai, H.; Uchimoto, Y.; Ogumi, Z. Delithiation/Lithiation Behavior of LiNi0.5Mn1.5O4 Studied by In Situ and Ex Situ Li6,Li7 NMR Spectroscopy. J. Phys. Chem. C 2015, 119, 13472−13480.
(24) Grenier, A.; Reeves, P. J.; Liu, H.; Seymour, I. D.; Marker, K.; Wiaderek, K. M.; Chupas, P. J.; Grey, C. P.; Chapman, K. W. Intrinsic Kinetic Limitations in Substituted Lithium-Layered Transition-Metal Oxide Electrodes. J. Am. Chem. Soc. 2020, 142, 7001−7011.